CHANNEL-TO-CHANNEL HEAT FLUX VARIATION IN COMPACT MINICHANNEL HEAT EXCHANGERS DUE TO THE EFFECT OF LOUVERED FINS

Khovalyg D.*, Hrnjak P. S., Jacobi A. M.
Author for correspondence
Department of Mechanical Science and Engineering
University of Illinois at Urbana-Champaign
Illinois, 61820
USA
E-mail: khovalyg@illinois.edu

ABSTRACT

A typical minichannel evaporator used in AC&R applications is made of stacked parallel aluminum extruded multiport plates and louvered fins placed between them. In this configuration cold refrigerant flows inside the ports, and hot air passes though the louvered fins. Heat flux variation between neighboring minichannels, in the direction from the leading to the trailing edge, may be expected since warmer air enters the louvered fins domain and its temperature is reduced at the outlet.

The possible nonuniformity of the heat flux from channel to channel was studied numerically using ANSYS Fluent as a three-dimensional time-dependent heat transfer problem of louvered fins bounded with multiport aluminum plates. While the fin geometry was kept constant in all simulations, two different multiport plate configurations (11 round ports, D = 1.2 mm; and 22 square ports, $0.54 \times 0.54\,\mathrm{mm}^2$) were analyzed at air face velocities from 1 m/s to 5 m/s. The wall temperature of all channels was set to be constant $10\,^o$C, which corresponds to the typical saturation temperature of refrigerants used in AC&R applications. The incoming air flow temperature considered was $20\,^o$C and $30\,^o$C.

Results illustrate that both air velocity and temperature play a profound role on heat flux variation from the leading to the trailing edge of the multichannel plate. The heat flux varies drastically in the case of the slower incoming air flow due to the significant change in the driving potential along the air flow, and it varies less at higher air velocities due to the heat transfer recovery effect behind the turning louver along with the smaller driving temperature difference between mixing cup and saturation temperature. The overall heat flux difference between the leading channel and the trailing one reaches almost 94% at free stream air velocity 1 m/s and 69% at air velocity of 5 m/s.

This numerical modeling of the conjugate heat transfer problem proves the presence of heat flux difference among channels which was overlooked in the literature. Understanding of the channel-to-channel heat flux variation is valuable for understanding the flow boiling behavior in parallel non-uniformly heated minichannels and the two-phase flow maldistribution.

NOMENCLATURE

T	[K]	Temperature
U	[m/s]	Velocity
D	[mm]	Diameter
L	[mm]	Length
q	[kW/m^2]	Heat flux
h	[W/m^2K]	Heat transfer coefficient
f	[Hz]	Frequency
Re	[-]	Reynolds number
St	[-]	Strouhal number

Special characters

Δ	[-]	Difference

Subscripts

air	air side
h	hydraulic
p	pitch (louver)

INTRODUCTION

Heat exchangers are key components of energy conversion systems, including air-conditioning and refrigeration equipment. The compact minichannel design of a heat exchanger (MCHX) allows for significant reduction of its volume, weight, and raw material in comparison to conventional fin-and-tube heat exchangers. MCHX are typically made of parallel aluminum extruded multiport plates and louvered fins such that refrigerant flows inside the ports and air flows over the fins in an unmixed cross flow configuration. Since refrigerant absorbs heat from the air, which cools off while passing through fins, heat flux variation between neighboring channels is expected. Studies by Khovalyg *et al.* [1; 2] showed the existence of the cross-correlation between parallel minichannels subjected to varying heat fluxes, and the most heated channel exhibits the profound role on flow maldistibution among parallel channels having a common manifold.

The flow field of multi-louvered fin arrays alone was extensively studied by Thole *et al.* [3; 4] and Tafti *et al.* [5; 6; 7]. They studied in detail, both numerically and experimentally, the effect of fins geometry on heat transfer, thermal wakes, onset and propagation of vortices, and transitional regimes. The air-side thermal-hydraulic performance of louvered fin heat exchangers was studied by Chang & Wang [8], Park & Jacobi [9; 10], An-

tonijevic [11], and Kang *et al.* [12]. In the work of Kang *et al.* [12] the flow and heat transfer characteristics of flat tube and multi-tube array coupled with louvered fins were investigated; however, they did not report tube-to-tube heat flux distribution for the multi-tube configuration.

Literature overview illustrates that there is a lack of research investigating the heat transfer across both louvered fins and multiport plates, and of reports on any channel-to-channel heat flux variations in compact heat exchangers. As a result, numerical simulations of the conjugate, three-dimensional, transient heat transfer problem through louvered fins bounded with multiport aluminum plates were performed. The possible nonuniformity of heat flux from channel to channel, typical in microchannel evaporators used in air-conditioning systems, was investigated using the commercial finite-volume-based CFD software ANSYS Fluent.

Quantification of the channel-to-channel heat flux variation can provide insight in understanding flow maldistribution between parallel minichannels and guide further analysis on flow boiling instabilities caused by non-uniform heat and mass flux distribution.

PROBLEM STATEMENT

The channel-to-channel heat flux variation is the result of two effects: transverse conduction from plates through thin louvered fins blown over by air flow, and longitudinal heat conduction within multiport aluminum plate along the air flow as shown in Figure 1.

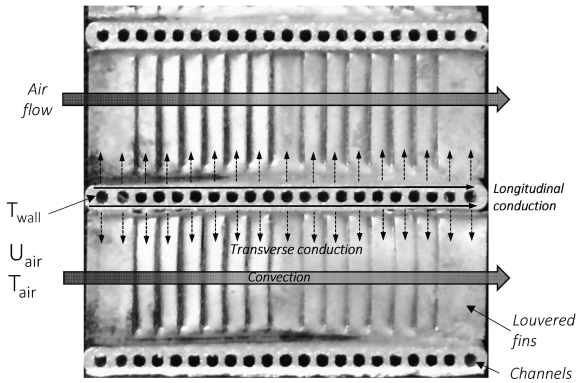

Figure 1. Heat transfer mechanisms (MCHX coss section)

The conjugate heat transfer problem for a set geometry can be solved by defining boundary conditions such as wall temperature of channels and incoming air flow temperature and velocity. For this reason, the constant wall temperature inside all channels was set at 10 °C. This temperature corresponds to the typical saturation temperature of refrigerants during flow boiling in minichannel evaporators used in air-conditioning application (*e.g.* R134a, R410A). The free stream air velocities were 1 m/s ($Re_{Lp} = 82$), 3 m/s ($Re_{Lp} = 246$) and 5 m/s ($Re_{Lp} = 410$), and they cover the range of air velocities in actual applications of MCHX. The temperature difference between the incoming air and the inside walls of the channels was taken as 10 K and 20 K, and the temperature of the incoming air was 20 °C and 30 °C respectively. Air was assumed to be incompressible with constant properties, negligible viscous dissipation and no buoyancy effects. Thermal conductivity of aluminum was taken as 180 W/(m K) corresponding to aluminum alloy 3003. It is assumed that fins and plates had negligible contact resistance.

The louvered fin configuration used in simulations represents a typical geometry used in practical applications, and its dimensions are illustrated in Figure 2. Two different configurations of aluminum plates shown in Figures 3 and 4 were examined. Plate **A** had 11 round ports and each port was 1.2 mm in diameter, and the overall height of the plate was 2.0 mm. Plate **B** had 22 square ports with hydraulic diameter 0.54 mm and plate height 1.04 mm. Both plate geometries were based on actual geometry of aluminum multiport plates. The louvered fin geometry was kept constant throughout two series of simulations in order to compare the effect of multichannel plate variation on the channel-to-channel heat flux distribution.

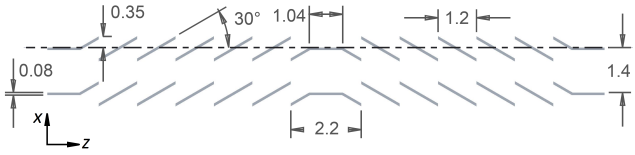

Figure 2. Louvered fins dimensions (cross sectional view)

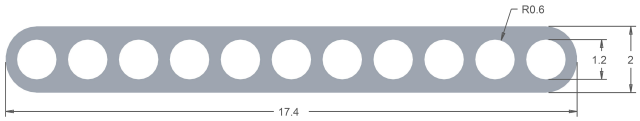

Figure 3. Multiport plate **A** dimensions

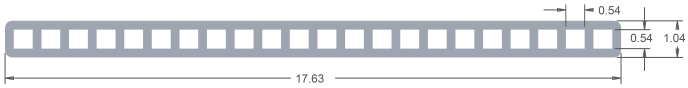

Figure 4. Multiport plate **B** dimensions

The geometry of the louvered fins was slightly simplified for numerical simulations: the curved edges of louvered fins near the fin root were ignored, and the un-louvered length at the fin root was slightly increased in order to obtain high quality meshing. Square channels were also adapted for the simulations: the round corners were ignored in order to reduce the number of small-scale cells that could complicate meshing and increase convergence time. The overview of the two considered configurations **A** and **B** are shown in Figure 5. Each configuration represented a repetitive unit of the microchannel heat exchanger, therefore symmetrical boundary conditions were introduced at the lower and upper surface of multichannel plates, and at the left and right surfaces.

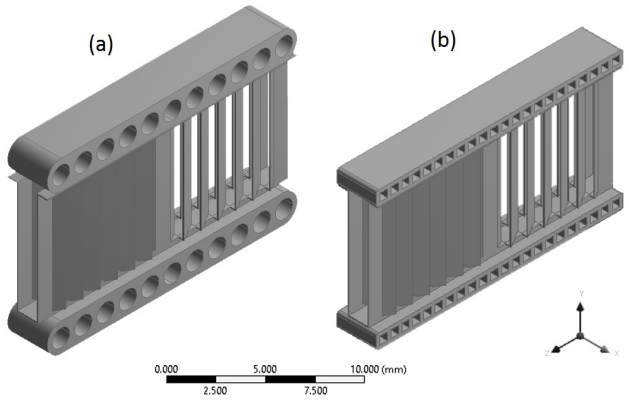

Figure 5. Overview of the two configurations: a) louvered fins with a plate **A**, b) louvered fins and a plate **B**

NUMERICAL METHOD

An unsteady laminar solution apporach was used to solve the problem since the flow was expected to become unsteady as velocity increases based on the numerical results of Tafti *et al.* [6]. They conducted numerical simulations on the air flow in a multi-louvered fin geometry at various Reynolds numbers and mapped the transition from steady to unsteady flow. According to the map, small recirculation zones are present at the exit wake of all louvers at Re_{Lp} number of 100, and the wake recirculation regions become larger as Re_{Lp} number increases. Separation and reattachment of shear layers at certain spots can be observed in the range of $Re_{Lp} = 200 - 400$. The wake of the exit louvers becomes unstable as Re_{Lp} number increases to 400, and the von Kármán vortex street is clearly present. In general, the flow is steady in the interior until Re_{Lp} number reaches 900.

Computational Domain

The computational domain had 2 zones (solid and fluid) and 4 major elements: fins, top and bottom multiport plates and air flow volume (Figure 6). In order to allow boundary layer development upstream of the first louver an air volume was extended upstream of the entrance louver, and an air flow volume was extended downstream of the exit louver such that a fully developed outflow boundary condition could be set at the outlet. The decision on the appropriate extension was undertaken after analyzing a few trial computations of the problem: it was observed that air accelerates at the inlet of the louvered fins domain and the free upstream velocity condition could not be set right at the beginning of the entrance lover. Similarly, unsteady wake behind the plate-and-fins domain forced to set the fully developed outflow condition far downstream from the exit louver. Additionally, symmetry conditions were imposed such as symmetry in Y-Z plane at the lower and upper surface of multichannel plates and air volume domains upstream and downstream; symmetry in X-Y plane at the left and right surfaces of the computational domain.

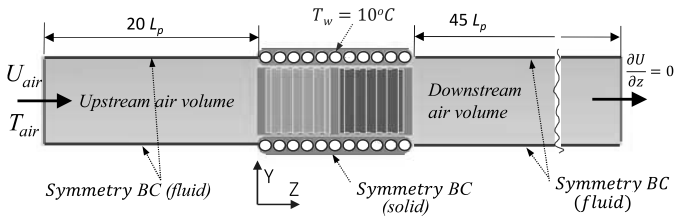

Figure 6. Computational domain and boundary conditions

Meshing

A tetrahedral fine conformal meshing was implemented throughout all the elements. The *Curvature and Proximity* size function was used to refine meshing around the corners, sharp edges, and narrow passages with a growth rate of 1.2 in addition to boundary layer refinement (5 layers). This resulted in about 3.3 million elements for the plate-and-fins configuration **A** and 9.3 million elements for configuration **B**. The average mesh quality was 0.838, and the standard deviation was no more than 0.1 for both configurations. A finer meshing for the second configuration was a result of the conformal meshing since a narrower multiport plate required finer meshing of its cross-section due to the thinner wall thickness.

The governing equations with the aforementioned boundary conditions were solved in the finite-volume based CFD software ANSYS Fluent. A *Pressure-Implicit with Splitting of Operators* (PISO) method was used for transient calculations since it is highly recommended for all transient flow calculations and for highly-distorted meshes without neighbor correction. The *second order upwind scheme* is used for the momentum and energy terms and *a second order accuracy* is obtained in the pressure term. Scaled residuals of continuity and momentum equations were set at 10^{-5} and energy equation converged at 10^{-8}.

Time Step

A time step of 5e-3 s (f=200 Hz) was chosen initially. Although the frequency of the vortex shedding from louvers in the current problem was expected to be 2 250 Hz at Re_{Lp}=82 and 11 250 Hz at Re_{Lp}=410 [13], the time step of was sufficient to resolve von Karman vortex sheet behind multiport plates. Numerical simulations were also performed with 1e-5 s time step (10 000 Hz), and results showed that time averaged heat fluxes does not differ significantly from the results calculated with the time step 5e-3 s. Moreover, a larger timescale allowed to perform simulations for a longer timeframe and examine possible presence of large scale heat flux fluctuations.

Validation Method

Results of the numerical simulations were compared against available results in the literature regarding the flow structure and air-side heat transfer coefficient. The work by Tafti *et al.* [6] was used to compare flow structures, and the Colburn j-factor correlation by Park and Jacobi [9] was used to evaluate heat transfer.

RESULTS AND DISCUSSION

Each channel was numbered starting from the leading edge, and heat flux coming through the inner wall surface of the multi-channel plate was used to compare the area averaged heat flux of each channel. The channel inner walls are split into *bottom* and *top* halves, and it is sufficient to define the heat flux field only for the halves of channels facing the fins due to the symmetry conditions imposed. Comparison of the channel-to-channel heat flux variation is provided for the area averaged heat flux taking into account both bottom and top sides of each channel.

Flow characteristics: velocity and temperature effect

The air flow was louver directed for each inlet velocity, while the wake behind louvers domain was stable at free stream air flow of U_{air}=1 m/s. The air flow exiting louvers domain had oscillating nature at U_{air}=3 m/s and U_{air}=5 m/s. Unstable outflow was caused by large-scale vortex shedding from plates in addition to the oscillations due to the merge of air streams from parallel louver banks.

Figure 7 provides an illustration of the velocity and temperature fields within the louvers domain. Contours are shown for the mid y-plane for configuration **A** at temperature difference ΔT = 20K and air velocities of U = 1 m/s (Figure 7a) and U = 5 m/s (Figure 7b). The air velocity varies from still up to 2.5 m/s (Figure 7a), and 13 m/s (Figure 7b) at set free stream velocities of 1 m/s and 5 m/s respectively. Additionally, airflow accelerates as it approaches the inlet of the louver domain. The actual velocity of the flow entering the louver banks is about 1.25 m/s and 6 m/s at set free stream velocities of 1 m/s and 5 m/s respectively.

Comparison of temperature fields at two flow velocities shows that flow at Re_{Lp} = 82 (U = 1 m/s) has a more uniform temperature behind the turning louver almost reaching the wall temperature of 283 K (10 °C) at the outlet. The air flow at Re_{Lp} = 410 (U = 5 m/s) is cooled only to 291 K (18 °C) at the outlet. Temperature fields are not affected much by the outflow oscillations; therefore, a little effect of the oscillating wake on the heat flux variation is expected.

Heat flux variation

Wall heat-flux contours are shown only for the configuration **A** at ΔT = 20K (Figure 8). Heat flux variation at ΔT = 10K was simillar, but the magnitude of the heat flux values was two times lower. Numerical results for the configuration **B** showed similar heat flux vartiation that occurred in a greater number of channels. In general, there was a slight difference in the heat flux field for the bottom and top sides due to the asymmetric orientation of the contact points between plates and louvers as shown in Figure 5. Top surface was joint to two parallel rows of louvers in the middle, while the bottom surface was connected to louvers at both edges.

The time and area averaged heat flux variation from channel to channel are illustrated in Figure 9 and 10. It is shown that the first channel, facing the flow, has the highest heat flux in all cases. The channel-to-channel heat flux for configuration **A** (Figure 9) was steadily decreasing from the leading channel to the last one

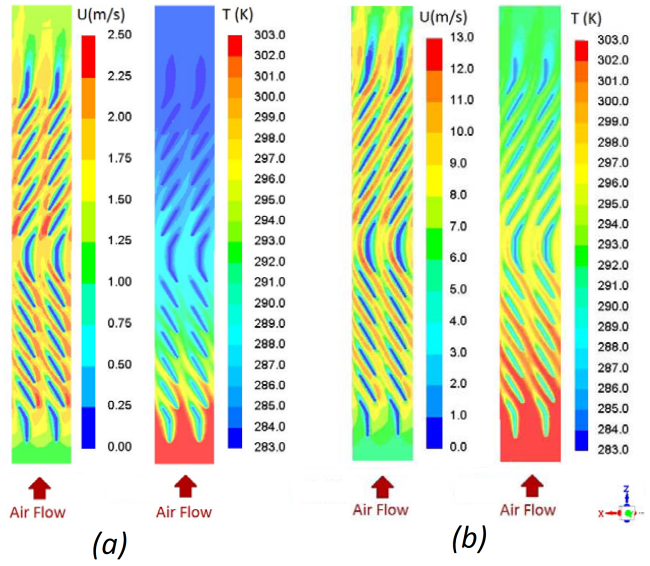

Figure 7. Velocity and temperature contours at ΔT = 20 K (configuration **A**, mid y-plane): (a) U = 1 m/s, (b) U = 5 m/s

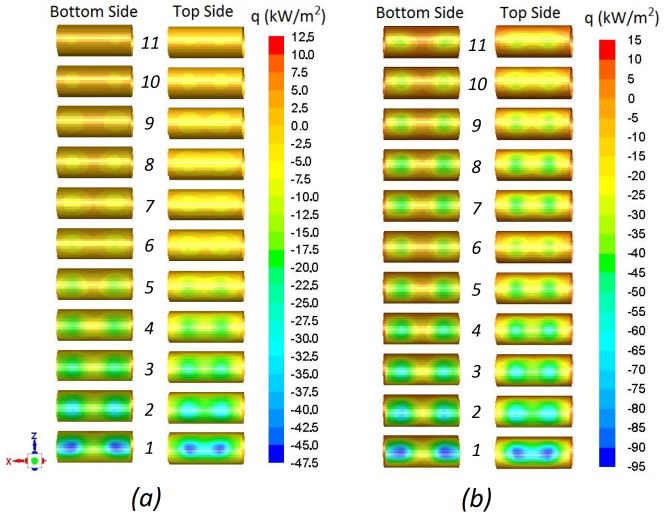

Figure 8. Heat flux contours at inner walls at ΔT = 20 K (configuration **A**, mid y-plane): (a) U = 1 m/s, (b) U = 5 m/s

at the lowest velocity U = 1 m/s, and the area averaged heat flux reduced 16 times from the leading channel to the last one. The channel-to-channel heat flux at velocities 3 m/s and 5 m/s for configuration **A** was also gradually decreasing in the upstream half region. The time averaged heat flux of channels 7 and 8, downstream of the turnaround louver, increased due to the air-side recovery zone formation behind the turn-around louver as air velocity increases. The area averaged heat flux dropped 4.2 times and 3.2 times from the leading channel to the last one at free stream air velocities U = 3 m/s and U = 5 m/s respectively.

The port-to-port heat flux distribution shown in Figure 10 for configuration **B**, which has higher number of smaller channels, was affected more by the growth of the boundary layer starting

from the leading edge of the plate. The 1^{st} channel exhibited the highest heat flux due to larger area exposed to the incoming hot air, while there was a 20% decrease in heat flux from the 1^{st} to the 2^{nd} channel due to less efficient heat transfer from the inlet louver. The heat flux of the 3^{rd} channel was recovered due to boundary layer separation starting at the 1^{st} louver. Apart from the aforementioned observation, the general behavior of the channel-to-channel heat flux distribution was similar to the configuration **A**. The heat transfer recovery effect behind the turning louver was spread over 4 channels (channels 13-16). The highest heat flux recovery effect was reached in channel 14: flux was recovered up to 7.2% at U = 3 m/s and 12.6% at U = 5 m/s. Overall, the area and time averaged heat flux lessened 24.5 times from the leading channel of plate **B** to the last one at free air stream velocity U = 1 m/s. In other words, heat flux of the 22^{nd} channel was 4.1% of that of the 1^{st} channel, and this is 53% higher than for the plate **A**. Heat flux reduced 5.2 times (19.1%) at U = 3 m/s, and 3.7 times (26.7%) at U = 5 m/s.

Generally, the channel-to-channel heat flux variation declines as free stream air velocity (higher Re_{Lp} numbers) increases due to the smaller change in mixing-cup temperature from inlet to outlet. Additionally, heat flux variation is significant at higher temperature difference between the channel wall and the incoming air stream ($\Delta T = 20K$ in the current study).

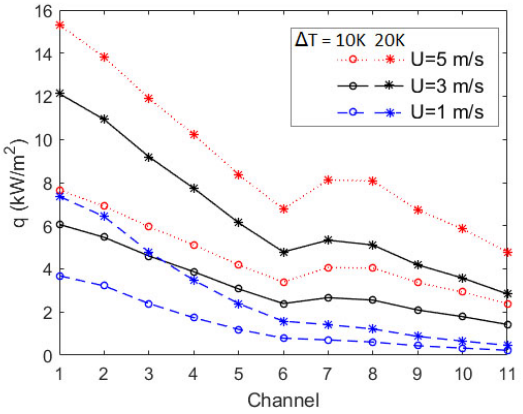

Figure 9. Time and area averaged heat flux per channel (configuration **A**)

Validation of Numerical Results

Current numerical results show a consistency with the findings by Tafti *et al.* [6]. There were no vortices observed from louvers and in the wake behind the exit from the heat exchanger for incoming air velocity of 1 m/s (Re_{Lp}=82). The air flow became unstable at incoming velocities of 3 m/s and 5 m/s, and there was vortex shedding at 5 m/s (Re_{Lp}=410) from the exit louvers and from the multichannel plates forming von Karman vortex street behind the heat exchanger. Small-scaled refined vortices were not observe in the current research since the time step chosen was 0.005 s (f=50 Hz) was not adequate to capture them. Interestingly, the current results show an interaction between outflow of two air streams from parallel row of louvers which has not

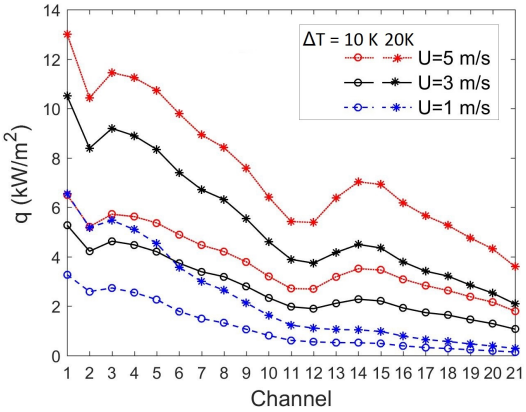

Figure 10. Time and area averaged heat flux per channel (configuration **B**)

been reported in the literature due to mainly focusing on a single row of fins. Flow instabilities observed at Re_{Lp}=410 in the current research are due to the shedding from the multiport plates typical to vortex shedding from bluff bodies.

The heat transfer coefficients for two limiting velocities (1 m/s and 5 m/s) determined based on numerical simulations are shown in Figure 11. Heat transfer is more efficient at smaller temperature difference of 10 K between the incoming flow and walls of the channels due to the more uniform temperature field; in addition, heat transfer is enhanced at higher air flow rate due to vortex generation resulting in better mixing. Heat transfer coefficients according to Park and Jacobi [9] correlation are 80.46 W/m^2K at U=1 m/s and 189.9 W/m^2K at U=5 m/s. The results show that prediction of the heat transfer coefficient for higher Reynolds number flow differs at most by 18% and as low as 7% for the configuration **A** and **B** at $U = 5$ m/s. Numerical results for heat transfer at lower velocity of $U = 1$ m/s is within 60% and as close as 36% for both geometries **A** and **B**.

Although non-dimensional heat transfer correltion by Park and Jacobi [9] was developed based on 1030 heat transfer experimental data points for flat-tube louver-fin heat exchangers collected from the literature and had a RMS residual of 11.5% [9], it exhibits discrepancy with numerical results, especially at low air velocities. The variations in predicting the heat transfer coefficient between low and higher Re_{Lp} could be explained by the contribution of the empirical coefficients listed in [9]in addition to the surface area that was used for the heat transfer evaluation. The entire surface area facing the fluid, including the edges of louvered fins, was taken into account in the numerical heat transfer calculation, while only face area of louvers is taken into account by Park and Jacobi. Overall, the comparison of heat transfer results against the correlation developed by Park and Jacobi shows a good agreement for high Re_{Lp} flow, while the correlation under-predicts Nu at lower incoming air velocity case.

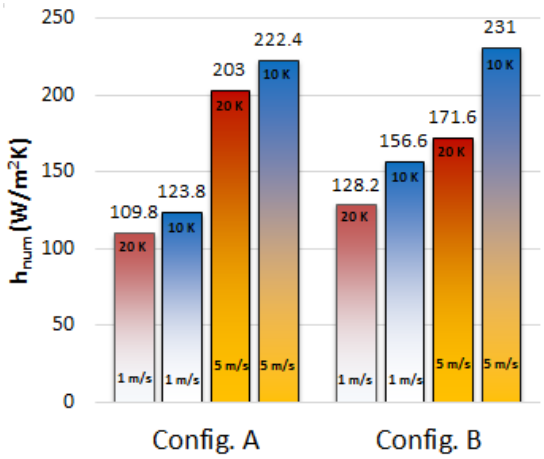

Figure 11. Heat transfer coefficient based on numerical results

CONCLUSION

Numerical results on heat flux variation show that the first channel, facing the flow, has the highest heat flux in all cases. The variation of the channel-to-channel heat flux downstream from the leading edge was dependent on the incoming flow velocity, temperature and air flow dynamics within louvered fins domain. The overall heat flux difference between the leading channel and the trailing one was 73% at the highest air velocity of $U = 5$ m/s, while this difference was almost 96% at the lowest velocity of $U = 1$ m/s for the plate with 22 square ports ($D_h = 0.54$ mm). The plate with 11 round ports (D = 1.2 mm) had a heat flux difference between the first and the last channel of 68.7% and 93.4% at $U = 5$ m/s and $U = 1$ m/s respectively. The magnitude of the heat flux difference at $\Delta T = 20$ K was twice as much as at $\Delta T = 10$ K.

In general, the heat flux distribution between neighboring channels is more uniform at increased incoming air stream velocity U and decreased temperature difference ΔT between channels wall and incoming air flow. The least variation in port-to-port heat flux distribution is observed at the highest incoming air velocity $U = 5$ m/s and the lowest temperature difference $\Delta T = 10$ K. Reduced heat flux variation at higher air velocity is due to the low change in the driving potential ($T_m - T_{sat}$) along the air flow in addition to the heat transfer recovery effect behind the turning louver. The highest heat recovery effect was observed at $U = 5$ m/s: 8.8% for configuration **A** and 12.6% for configuration **B**. The heat flux between the leading and the trailing edge of the multichannel plate varies drastically in the case of the slower (1 m/s) incoming air flow. Oppositely, a higher air velocity (mass flow rate) corresponds to a lower temperature drop for the air stream, and less variation in the temperature driving potential (port-to-port) causes less heat flux variation.

In conclusion, numerical simulations results prove the presence of heat flux difference among channels which was overlooked in the literature. In addition, the results of this work can be utilized in analyzing possible effect of heat flux variation on flow boiling instabilities between neighboring microchannels and the two-phase flow maldistribution.

REFERENCES

[1] Dolaana M Khovalyg, Pega S Hrnjak, and Anthony M Jacobi. Transient pressure drop cross-correlation during flow boiling of r134a in parallel minichannels. *Science and Technology for the Built Environment*, 21(5):545–554, 2015.

[2] Dolaana Khovalyg, Predrag S Hrnjak, and Anthony M Jacobi. Interactions between parallel unevenly heated minichannels during flow boiling of r134a. *Heat Transfer Engineering*, 37(11):921–937, 2016.

[3] Marlow E Springer and Karen A Thole. Experimental design for flowfield studies of louvered fins. *Experimental Thermal and Fluid Science*, 18(3):258–269, 1998.

[4] Marlow E Springer and Karen A Thole. Entry region of louvered fin heat exchangers. *Experimental Thermal and Fluid Science*, 19(4):223–232, 1999.

[5] X Zhang and DK Tafti. Classification and effects of thermal wakes on heat transfer in multilouvered fins. *International Journal of Heat and Mass Transfer*, 44(13):2461–2473, 2001.

[6] DK Tafti, G Wang, and W Lin. Flow transition in a multilouvered fin array. *International journal of heat and mass transfer*, 43(6):901–919, 2000.

[7] DK Tafti and J Cui. Fin–tube junction effects on flow and heat transfer in flat tube multilouvered heat exchangers. *International Journal of Heat and Mass Transfer*, 46(11):2027–2038, 2003.

[8] Yu-Juei Chang and Chi-Chuan Wang. A generalized heat transfer correlation for iouver fin geometry. *International Journal of heat and mass transfer*, 40(3):533–544, 1997.

[9] Young-Gil Park and Anthony M Jacobi. Air-side heat transfer and friction correlations for flat-tube louver-fin heat exchangers. *Journal of Heat Transfer*, 131(2):021801, 2009.

[10] Young-Gil Park and Anthony M Jacobi. The air-side thermal-hydraulic performance of flat-tube heat exchangers with louvered, wavy, and plain fins under dry and wet conditions. *Journal of heat transfer*, 131(6):061801, 2009.

[11] Dragi Antonijevic. An engineering procedure for air side performance evaluation of flat tube heat exchangers with louvered fins. *Heat and Mass Transfer*, 49(1):117–127, 2013.

[12] Hie Chan Kang, Hyejung Cho, Jin Ho Kim, and Anthony M Jacobi. Air-side heat transfer performance of louver fin and multitube heat exchanger for direct methanol fuel cell cooling application. *Journal of Fuel Cell Science and Technology*, 11(4):041004, 2014.

[13] NC DeJong, LW Zhang, AM Jacobi, S Balachandar, and DK Tafti. A complementary experimental and numerical study of the flow and heat transfer in offset strip-fin heat exchangers. *Journal of heat transfer*, 120(3):690–698, 1998.